

Spatial Reconstructed Local Attention Res2Net with F0 Subband for Fake Speech Detection[★]

Cunhang Fan^a, Jun Xue^a, Jianhua Tao^b, Jiangyan Yi^c, Chenglong Wang^c, Chengshi Zheng^d and Zhao Lv^a

^aAnhui Province Key Laboratory of Multimodal Cognitive Computation, School of Computer Science and Technology, Anhui University, Hefei, 230601, China

^bDepartment of Automation, Tsinghua University, Beijing, 100190, China

^cNational Laboratory of Pattern Recognition, Institute of Automation, Chinese Academy of Sciences, Beijing, 100190, China

^dKey Laboratory of Noise and Vibration Research, Institute of Acoustics, Chinese Academy of Sciences, Beijing, 100190, China

ARTICLE INFO

Keywords:

ASVspoof
fake speech detection
fundamental frequency
Res2Net

ABSTRACT

The rhythm of synthetic speech is usually too smooth, which causes that the fundamental frequency (F0) of synthetic speech is significantly different from that of real speech. It is expected that the F0 feature contains the discriminative information for the fake speech detection (FSD) task. In this paper, we propose a novel F0 subband for FSD. In addition, to effectively model the F0 subband so as to improve the performance of FSD, the spatial reconstructed local attention Res2Net (SR-LA Res2Net) is proposed. Specifically, Res2Net is used as a backbone network to obtain multiscale information, and enhanced with a spatial reconstruction mechanism to avoid losing important information when the channel group is constantly superimposed. In addition, local attention is designed to make the model focus on the local information of the F0 subband. Experimental results on the ASVspoof 2019 LA dataset show that our proposed method obtains an equal error rate (EER) of 0.47% and a minimum tandem detection cost function (min t-DCF) of 0.0159, achieving the state-of-the-art performance among all of the single systems.

1. Introduction

Automatic speaker verification (ASV) technology has become increasingly mature, but it remains vulnerable to attack by existing synthetic speech techniques. Generally, fake speech can be divided into three types: audio playback Ali, Sabir and Hassan (2021); Hajipour, Akhaee and Toosi (2021); Kinnunen, Sahidullah, Delgado, Todisco, Evans, Yamagishi and Lee (2017a); Kinnunen, Sahidullah, Falcone, Costantini, Hautamäki, Thomsen, Sarkar, Tan, Delgado, Todisco et al. (2017b); Paul, Das, Sinha and Prasanna (2016); Shang and Stevenson (2008), text-to-speech (TTS) Huang, Lin, Liu, Chen and Lee (2022); Shchemelinin, Vadim and Simonchik (2013); Zhang, Gu, Yi and Zhao (2022), and voice conversion (VC) Chen, Kumar, Nagarsheth, Sivaraman and Khoury (2020); Kinnunen, Wu, Lee, Sedlak, Chng and Li (2012); Tian, Lee, Wu, Chng and Li (2017). In order to reduce the risk of spoofing attacks on ASV caused by fake audio, the ASVspoof challenges have been held successively in 2015 Wu, Kinnunen, Evans, Yamagishi, Haniłçi, Sahidullah and Sizov (2015), 2017 Kinnunen et al. (2017a), 2019 Todisco, Wang, Vestman, Sahidullah, Delgado, Nautsch, Yamagishi, Evans, Kinnunen and Lee (2019), and 2021 Yamagishi, Wang, Todisco, Sahidullah, Patino, Nautsch, Liu, Lee, Kinnunen, Evans et al. (2021). In 2022, the Audio Deep Synthesis Detection (ADD 2022) Yi, Fu, Tao, Nie, Ma, Wang, Wang, Tian, Bai, Fan et al. (2022) was also successfully held. Currently, the

main focus of research in fake speech detection (FSD) lies in the design of front-end features and back-end models.

For front-end features, many acoustic features are investigated Das, Yang and Li (2019); Doan, Nguyen-Vu, Jung and Hong (2023); Huang, Cui, Huang and Kang (2023); Li, Wang, He, Abdullahi and Li (2022); Paul, Pal and Saha (2017); Sanchez, Saratxaga, Hernaez, Navas, Erro and Raitio (2015); Wei, Long, Wei and Li (2022); Williams and Rownicka (2019); Yang and Das (2020); Yang, Das and Zhou (2019b), such as Mel Frequency Cepstral Coefficients (MFCC), constant Q cepstral coefficients (CQCC), linear frequency cepstral coefficients (LFCC) and so on. In addition, in Witkowski, Kacprzak, Zelasko, Kowalczyk and Galka (2017), it is proposed to use Inverse MFCC (IMFCC), Linear Prediction Cepstral Coefficients (LPCC), and LPCCres¹ features. Then, the high-frequency components of these three features are fed to a classifier that classifies real samples and replayed samples. In Chettri, Kinnunen and Benetos (2020a), it is proposed to divide the whole frequency band into multiple disjoint sub-bands. And a joint subband modeling architecture is designed to learn the specific features of subbands. In Zhang, Wang and Zhang (2021b), it is proposed to divide the log power spectrogram (LPS) feature frequency band into two frequency bands, namely high frequency and low frequency. Based on the results of the experiments, low frequency has superior performance to high frequency. While these methods make significant advances in FSD and demonstrate that different

[★]Corresponding author: Zhao Lv and Jianhua Tao.

✉ jhtao@tsinghua.edu.cn (J. Tao); kjlz@ahu.edu.cn (Z. Lv)
ORCID(s):

¹Proposed by the authors of Witkowski et al. (2017), and derived by the LPCC.

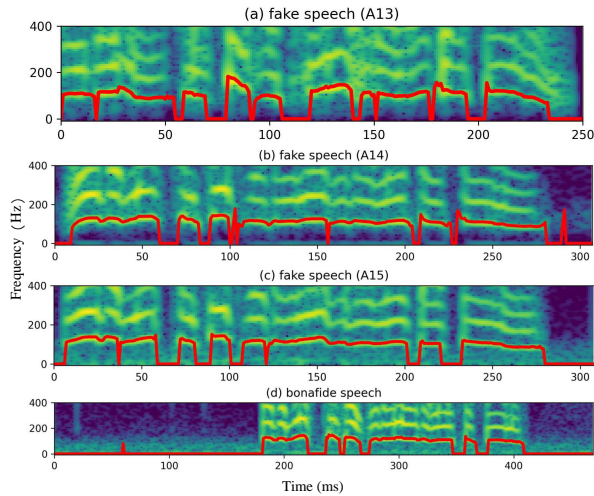


Figure 1: The spectrum and F0 distribution of three different types fake speech and the corresponding bonafide speech. Where the red line means the distribution of F0. A13, A14 and A15 denote three different TTS algorithms drawn from the ASVspoof 2019 LA dataset, as described in Wang et al. (2020b).

frequency bands have different effects, they do not specify how the bands should be divided.

For back-end models, deep neural network (DNN) Jung, Heo, Tak, Shim, Chung, Lee, Yu and Evans (2022); Kim and Ban (2023) classifiers can acquire impressive results for FSD task. The ResNet He, Zhang, Ren and Sun (2016) architecture, which has been successful in the image field He, Xu, Zhang and Zhu (2023); Sun, Ding and Guo (2022), has strong feature capture capabilities. Therefore, in Ling, Huang, Huang, Zhang and Li (2021); Zhang, Jiang and Duan (2021a); Zhang et al. (2021b), authors propose a series of ResNet-based classifiers to detect fake speech. To further enhance the generalization capability of the model, Gao et al. Gao, Cheng, Zhao, Zhang, Yang and Torr (2019) propose the Res2Net structure, which partitions channels into multiple groups and enables interaction through residual connections within each group to extract multi-scale features. Consequently, researchers Li, Li, Weng, Liu, Su, Yu and Meng (2021a); Li, Wu, Lu, Liu and Meng (2021b) have made many beneficial attempts to use the Res2Net architecture for the FSD task. However, the residual connections directly add information from the previous channel group to the next, and research Li et al. (2021b) has shown that the cross-channel information can generate redundant information. Therefore, after aggregating information from multiple channel groups in Res2Net, the salient discriminative features may be interfered with by redundant information. These issues limit the performance of the FSD system.

Recent research in text-to-speech (TTS) has indicated that the fundamental frequency (F0) is very important for the quality of synthetic speech. For example, in Łańcucki (2021), a new TTS model Fastpitch is proposed to predict

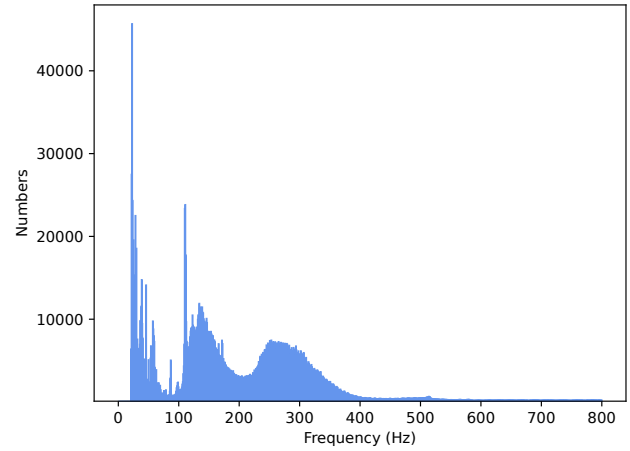


Figure 2: The frequency of F0 distribution in the ASVspoof 2019 LA training dataset. Where the abscissa is the frequency corresponding to F0, and the ordinate is the number of F0 at this frequency.

the F0 contour during inference. Changed predictions make the generated speech more human-like. However, it is worth noting that the rhythm of synthetic speech is usually too smooth, which leads to the F0 of synthetic speech being very different from the F0 of real speech. In order to compare the F0 distribution of fake speech and bonafide speech, Fig. 1 shows the spectrum and F0 distribution of three different fake voices and one bonafide speech, with the red line depicting the distribution of F0. From Fig. 1 we can find that the F0 distribution of these three different types fake speech is distinctly different from the corresponding bonafide speech. This indicates that the F0 feature contains the discriminative information for the FSD task.

Unfortunately, F0 cannot be used as input feature, since it consists of only one dimension. In order to make full use of the discriminative information of F0, this paper proposes a F0 subband for FSD task, which is the subband of amplitude spectrum. Fig. 2 shows the F0 distribution in the ASVspoof 2019 LA training dataset. From Fig. 2 we can find that most of the F0 is distributed between 0-400 Hz. Therefore, the frequency band containing most of the F0 is used as the F0 subband. In addition, to effectively model the F0 subband, we propose a novel spatial reconstructed local attention Res2Net (SR-LA Res2Net) for FSD. Specifically, the Res2Net is used as the backbone network, which can capture the multi-scale information of the input feature. However, the gradual superposition of cross-channel group information will cause more artifacts to the spatial structure of the feature, and the redundant information generated by aggregation may obscure some important information. In order to address these problems, we design a spatial reconstructed (SR) block at the residual connection in Res2Net, which is used to reconstruct the spatial structure. Finally, the local attention (LA) block is integrated at the bottom of Res2Net to focus on local information and capture the discriminative information of F0 subband.

The main contributions of this study can be summarized as two-fold. Firstly, we propose to use the F0 subband for the FSD task, which is a very discriminative feature. Secondly, a novel SR-LA Res2Net architecture is designed to model the F0 subband, which can effectively solve the shortcomings of Res2Net when expanding feature receptive fields. The experimental results on the ASVspoof 2019 LA dataset show that our proposed method is very effective for the FSD task, and it can acquire the state-of-the-art performance among all of the single systems.

The rest of this article is arranged as follows. Section II introduces the related works. The proposed method is introduced in section III. Experiments and results are given in section IV. Section V shows the discussions. Section VI draws conclusions.

2. Related Works

For the FSD task, many studies Chettri, Kinnunen and Benetos (2020b); Yang, Das and Li (2019a); Zhang, Yi and Zhao (2021c) have shown that different frequency bands have different effects. In Zhang et al. (2021b), the authors focus on global channel attention using squeeze and extraction blocks and explore the impact of high frequency and low frequency subband for the FSD task. The low frequency subband achieves good performance. In Ling et al. (2021), the authors propose a frequency attention block and a channel attention block, which pays attention to the basic subband correlation and channel relationship, respectively.

In addition, many studies Jung et al. (2022); Lv, Zhang, Tang and Hu (2022); Tak, weon Jung, Patino, Todisco and Evans (2021a); Tak, Jung, Patino, Kamble, Todisco and Evans (2021b) are based on the Res2Net for FSD and acquire quite good performances. In Li et al. (2021a), the authors use Res2Net to enhance the system's generalization to unseen spoofing attacks, and integrate squeeze and extract blocks to further improve performance. In Li et al. (2021b), the authors propose a channel-wise gated Res2Net (CG-Res2Net), which dynamically adjusts the correlation between channels through a gating mechanism and suppresses channels with small correlations. It further enhances the generalization ability of the system against unseen spoofing attacks.

In this paper, we propose the F0 subband and SR-LA Res2Net for FSD. Compared with Res2Net and CG-Res2Net, the proposed SR-LA Res2Net has better generalization ability.

3. The Proposed F0 Subband with SR-LA Res2Net

In this paper, we propose a F0 subband with SR-LA Res2Net for FSD. Because the F0 of synthetic speech is very different from the real one. Therefore, we think the F0 contains the discriminative information and apply the F0 subband as the input feature for FSD. To further improve the performance of FSD, we propose the SR-LA Res2Net to model the F0 subband feature, which can effectively

solve the shortcomings of Res2Net when expanding feature receptive fields.

3.1. F0 Subband

In order to make full use of the discriminative information of F0, we extract the F0 subband based on the LPS. Specifically, the short-time Fourier transform (STFT) is used to convert the time domain raw waveform $\mathbf{x}[k]$ into the time-frequency (T-F) domain.

$$\mathbf{X}_r[t, f] + j \cdot \mathbf{X}_i[t, f] = STFT(\mathbf{x}[k]) \quad (1)$$

where k is the time index of raw waveform $\mathbf{x}[k]$. $STFT$ means the operation of STFT. $\mathbf{X}_r \in \mathbb{R}^{F \times T}$ and $\mathbf{X}_i \in \mathbb{R}^{F \times T}$ are the corresponding real and imaginary part of STFT, respectively. t is the index of time frame and f is the index of frequency bin. F and T are the number of frequency bins and time frames, respectively. For convenience, (t, f) is omitted from the following formulas in this paper.

The full frequency bands of LPS_{full} can be acquired as follows:

$$LPS_{full} = \log \sqrt{(\mathbf{X}_r)^2 + (\mathbf{X}_i)^2} \in \mathbb{R}^{F \times T} \quad (2)$$

From Fig. 2 we can find that most of the F0 is distributed between 0-400 Hz. Therefore, the 0-400 Hz of LPS is applied as our F0 subband LPS_{F0} .

$$LPS_{F0} = LPS_{0-400 \text{ Hz}} \quad (3)$$

3.2. Model Architecture

In order to effectively model the F0 subband and improve the performance of FSD, we propose the SR-LA Res2Net architecture. Fig. 3 shows the schematic diagram of the proposed SR-LA Res2Net architecture. Firstly, to extract the multi-scale information of the F0 subband, the Res2Net is used as the backbone. However, when the channel group is constantly superimposed, the Res2Net may generate redundant information so that much important information may be lost. To address this issue, the SR block is proposed at the residual connection between channel groups, which can restore the spatial structure. In addition, a LA block is designed at the bottom of Res2Net to pay attention to local information and remove the influence of redundant information. Therefore, our proposed SR-LA Res2Net can further remove spatial artifacts and redundant information while extracting multi-scale features, thereby improving the generalization ability of the model to unseen spoofing attacks.

3.2.1. The Res2Net Architecture

The ResNet has been applied in various fields as soon as it was proposed and has achieved great performance. Even if ResNet's residual connections can reduce the impact of network depth, just increasing the network depth does not improve the performance of the model very well. So Gao et al. Gao et al. (2019) proposed the Res2Net architecture, which obtains multi-scale features through the information transfer of channel groups. Firstly, to expand the range of

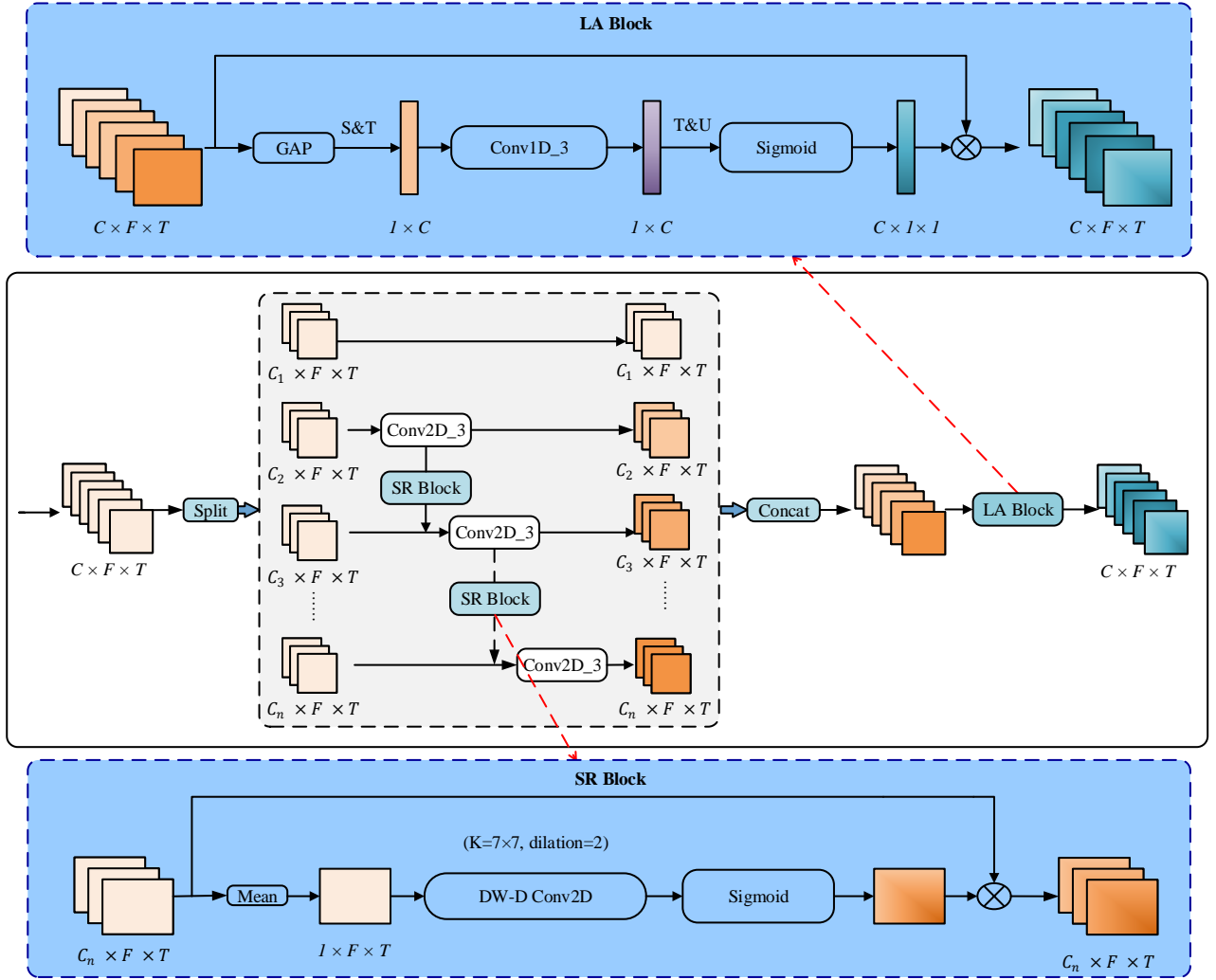


Figure 3: The schematic diagram of the proposed SR-LA Res2Net architecture. The spatial reconstructed (SR) block is used to remove the spatial structure artifacts of the channel group, and the local attention (LA) block aims to highlight important information and remove redundant information.

interaction between channel groups, the input features are divided into n subsets according to the channel dimension after 1×1 convolution, denoted as s_i , where $i \in \{1, 2, \dots, n\}$. As for s_1 , it does not undergo any processing. And as for s_2 , it is directly output after a 3×3 convolution $K_2(\cdot)$. As for s_3 to s_n , each s_i needs to be added to the output of K_{i-1} before passing through $K_i(\cdot)$. This process can be formulated as follows:

$$y_i = \begin{cases} s_i, & i = 1 \\ K_i(s_i), & i = 2 \\ K_i(s_i + y_{i-1}), & 3 \leq i \leq n \end{cases} \quad (4)$$

where n is defined as the scale dimension, indicating the number of channel groups applied to split feature maps.

Therefore, the Res2Net can increase the interaction between channel groups through residual connections in the block. Through the residual connections in the block, each channel group obtains a different amount of information,

thereby it can generate multiple-scale features. Such a multi-scale representation increases the receptive field. Finally, all channel groups are aggregated and the original channel size is maintained by the 1×1 convolution.

3.2.2. SR Block

The Res2Net has a strong feature representation ability, which relies on the information transfer of multiple internal channel groups. However, as the feature information continues to be superimposed, more artifacts will appear in its spatial structure. This greatly affects the performance of the Res2Net model. Inspired by Woo, Park, Lee and Kweon (2018), we design a SR block for residual connection between channel groups. It aims to reconstruct the feature space and remove its artifacts when the information is passed to the next channel group.

Table 1

The detailed information of ASVspoof 2019 LA Dataset. Where the "utt." means the number of utterance.

Partition	Bonafide	Spoof	Spoof
	utt.	utt.	attacks type.
Train.	2580	22800	A01-A06
Dev.	2548	22296	A01-A06
Eval.	7355	63882	A07-A19

Firstly, to reduce subsequent parameter computations, we compress the channel dimension:

$$\mathcal{F}_{\text{Mean}} \in \mathbb{R}^{1 \times F \times T} = \text{Mean}(\mathcal{F}_{\text{in}} \in \mathbb{R}^{C \times F \times T}) \quad (5)$$

where $\text{Mean}(\cdot)$ means the mean operation, \mathcal{F}_{in} is the input feature, and C is the number of channels.

Then, to further expand the receptive field, the depth-wise dilation convolution is applied:

$$\mathcal{F}_{\text{DW-DC}} \in \mathbb{R}^{1 \times F \times T} = \text{DW-DC}(\mathcal{F}_{\text{Mean}} \in \mathbb{R}^{1 \times F \times T}) \quad (6)$$

where DW-DC represents the operation of depth-wise dilation convolution.

Finally, $\mathcal{F}_{\text{DW-DC}} \in \mathbb{R}^{1 \times F \times T}$ reconstructs the feature space through the sigmoid layer. Then it multiplies with the input feature \mathcal{F}_{in} :

$$\mathcal{F}_{\text{sr}} \in \mathbb{R}^{C \times F \times T} = \mathcal{F}_{\text{in}} \otimes \text{sigmoid}(\mathcal{F}_{\text{DW-DC}} \in \mathbb{R}^{1 \times F \times T}) \quad (7)$$

where \mathcal{F}_{sr} represents the reconstructed feature space. \otimes denotes the element-wise multiplication.

3.2.3. LA Block

Although Res2Net can obtain multi-scale global information, due to the uneven interaction information between the channel groups, this uneven global interaction may lead to information redundancy and the useful information may not be focused. To address this problem, motivated by Wang, Wu, Zhu, Li, Zuo and Hu (2020a), the LA block is applied to focus on the local information.

Firstly, the global average pooling (GAP) is used to squeeze the dimensions of the input features:

$$\mathcal{F}_{\text{GAP}} \in \mathbb{R}^{C \times 1 \times 1} = \text{GAP}(\mathcal{F}_{\text{g}} \in \mathbb{R}^{C \times F \times T}) \quad (8)$$

Where $\text{GAP}(\cdot)$ represents a GAP operation, \mathcal{F}_{g} is the output of Res2Net feature aggregation.

In order to squeeze the one-dimensional channel of the convolution, squeeze and transpose operations are then applied:

$$\mathcal{F}_{\text{S\&T}} \in \mathbb{R}^{1 \times C} = \text{S\&T}(\mathcal{F}_{\text{GAP}} \in \mathbb{R}^{C \times 1 \times 1}) \quad (9)$$

where $\text{S\&T}(\cdot)$ means the operation of squeeze and transpose.

In Hu, Shen, Albanie, Sun and Wu (2019), the authors proposed the Squeeze-and-Excitation (SE) block, which is different from the LA block in that they use two fully-connected layers to learn global channel attention. The first

FC layer is used for dimensionality reduction, and the second FC layer is used to restore the dimensionality. Although the parameters of this method are reduced by the dimensionality reduction, the complexity of the model is still very high. In addition, the dimensionality reduction can affect the performance of the model. In order to address this issue, motivated by Wang et al. (2020a), we apply the one-dimensional convolution to acquire the local attention information. The details are as follows:

$$\mathcal{F}_{\text{Conv}} = \text{Conv}(\mathcal{F}_{\text{S\&T}} \in \mathbb{R}^{1 \times C}) \quad (10)$$

where the $\text{Conv}(\cdot)$ is the operation of one-dimensional convolution.

Then, the feature size is gradually restored by the transpose and unsqueeze operations, which is defined as follows:

$$\mathcal{F}_{\text{T\&U}} \in \mathbb{R}^{C \times 1 \times 1} = \text{T\&U}(\mathcal{F}_{\text{Conv}} \in \mathbb{R}^{1 \times C}) \quad (11)$$

where $\text{T\&U}(\cdot)$ means the operation of transpose and unsqueeze.

Finally, the $\mathcal{F}_{\text{T\&U}} \in \mathbb{R}^{C \times 1 \times 1}$ is passed by the sigmoid layer to acquire the vector of attention weight. And the finally local attention vector can be obtained by multiplying the attention weight and the input feature \mathcal{F}_{g} of local attention block.

$$\mathcal{F}_{\text{la}} = \mathcal{F}_{\text{g}} \otimes \text{sigmoid}(\mathcal{F}_{\text{T\&U}} \in \mathbb{R}^{C \times 1 \times 1}) \quad (12)$$

where the \mathcal{F}_{la} denotes the output of local attention block.

4. Experiments and Results

4.1. Dataset

We conduct our experiments on the ASVspoof 2019 LA database and the ASVspoof 2021 LA database.

4.1.1. ASVspoof 2019 LA Database

ASVspoof 2019 LA mainly has 19 spoofing attack algorithms (A01-A19), including three types of spoofing attacks: TTS, voice conversion (VC), and audio playback. Table 1 details the components of the ASVspoof 2019 LA dataset. It can be seen that the LA subset has three parts: training, development, and evaluation. Among them, the training set is used to train the model, the development set is used to select the best performing model in training, and finally, the model performance is evaluated through the evaluation set. The training set and development set mainly include four TTS and two VC algorithms, namely A01-A06. To better evaluate the performance of the system, unseen spoofing attacks were added to the evaluation set, including two known spoofing attacks (A16 and A19) and 11 unseen spoofing attacks (A07-A15, A17, and A18).

4.1.2. ASVspoof 2021 LA Database

The difference of ASVspoof 2019 and 2021 LA database is the evaluation set. Therefore, the ASVspoof 2019 LA training and dev sets are used to train the model. The

Table 2

The proposed SR-LA Res2Net model architecture and configuration. Dimensions refer to (channels, frequency, and time). Batch normalization (BN) and Rectified Linear Unit (ReLU), SR and LA are the spatial reconstruction block and the local attention block, respectively.

Layer	Input: 27000 samples	Output shape
Front-end	F0 subband	(45,600)(F,T)
Post-processing	Add channel	(1,45,600)
	Conv2D_1 BN & ReLU	(16,45,600)
Res2-block	$2 \times \left\{ \begin{array}{l} \text{Conv2D_1} \\ \text{Conv2D_3 \& SR} \\ \text{Conv2D_1} \\ \text{LA} \end{array} \right\}$	(32,45,600)
Res2-block	$2 \times \left\{ \begin{array}{l} \text{Conv2D_1} \\ \text{Conv2D_3 \& SR} \\ \text{Conv2D_1} \\ \text{LA} \end{array} \right\}$	(64,23,300)
Res2-block	$2 \times \left\{ \begin{array}{l} \text{Conv2D_1} \\ \text{Conv2D_3 \& SR} \\ \text{Conv2D_1} \\ \text{LA} \end{array} \right\}$	(128,12,150)
Res2-block	$2 \times \left\{ \begin{array}{l} \text{Conv2D_1} \\ \text{Conv2D_3 \& SR} \\ \text{Conv2D_1} \\ \text{LA} \end{array} \right\}$	(256,6,75)
Output	Avgpool2D(1,1) AngleLinear	(256,1,1) 2

evaluation set contains about 180,000 utterances transmitted through real telephone systems with different bandwidths and different codecs. The transmission interference of this data set greatly affects the performance of the FSD system and makes it more challenging.

To quantitatively evaluate the performance of different FSD systems, EER and the minimum normalized tandem detection cost function (min t-DCF) are applied. EER is the working point where the false rejection rate (FRR) and false acceptance rate (FAR) are equal.

4.2. Experimental Setup

For the experiments of our proposed method, we apply the F0 subband as our input feature. First, we do STFT operation on the raw audio waveform. We use Blackman as the window function of STFT, and set the window length and hop length to 1728 and 130, respectively, to obtain a spectrogram with a size of 865. Then, we fix the number of frames at 600 by truncating and concatenating. Finally, it can be seen from Fig. 2 that the main distribution interval of F0 is 0-400 Hz. Therefore, we use the 0-400 Hz LPS feature as our F0 subband, and we take the first 0-45 dimension as the F0 subband feature, and the resulting F0 subband feature size is 45×600.

In this paper, we propose SR-LA Res2Net as a deep neural network classifier. Table 2 illustrates the architecture of SR-LA Res2Net, including convolution kernels, channels, and repeat times. In addition, in all experiments in this paper,

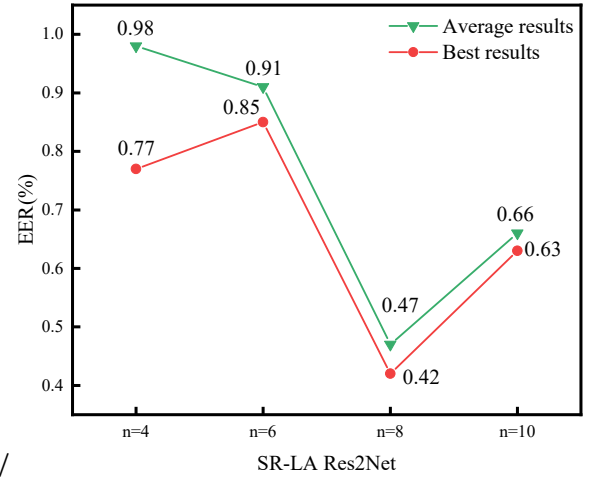


Figure 4: The EER results of SR-LA Res2Net for different number of channel groups (n). To avoid randomness in the experiments, the results are averaged for the three runs. Where the green line means the average results and the red line denotes the the best results of the three runs.

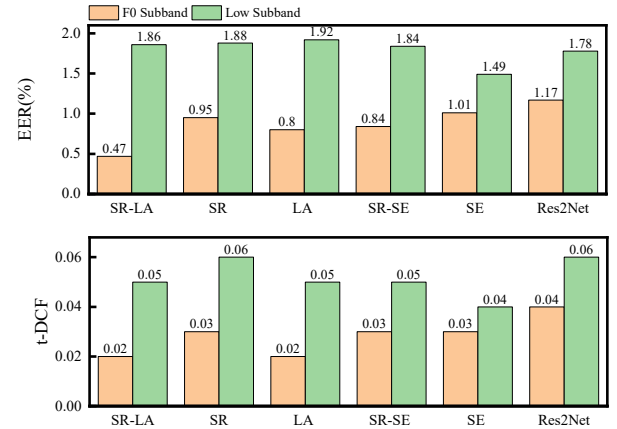


Figure 5: The EER and t-DCF results for we proposed different systems in the ASVspoof 2019 LA evaluation set (A07-A19). Where SR, LA, and SE are the different components embedded in the Res2Net.

we use Adam as the optimizer, and the parameters of the optimizer are set to: $\beta_1 = 0.9$, $\beta_2 = 0.98$, $\epsilon = 10^{-9}$ and weight decay 10^{-4} . The number of the epoch is 32. Fig. 4 shows the EER results for different number of channel groups (n) based on the SR-LA Res2Net architecture. From Fig. 4, we can see that the best performance is achieved for n=8, so we set the number of channel groups to 8 in the experiment.

In addition, since the ASVspoof 2021 LA dataset was interfered with by transmissions such as telephone communications, we used the RawboostTak, Kamble, Patino, Todisco and Evans (2022) data enhancement method when training the evaluation used for the ASVspoof 2021 LA dataset. Specifically, we added impulse signal-independent additive noise and stationary signal-independent additive noise to the original waveform.

Table 3

Results of our proposed ablation experiments for different components. The results are the average of three runs, with the best of the three results in parentheses.

Systems	t-DCF	EER(%)
SR-LA Res2Net (F0)	0.0159(0.0143)	0.47(0.42)
SR-SE Res2Net (F0)	0.0270(0.0227)	0.84(0.74)
SR Res2Net (F0)	0.0306(0.0302)	0.96(0.95)
LA Res2Net (F0)	0.0246(0.0229)	0.80(0.77)
SE Res2Net (F0)	0.0310(0.0292)	1.01(0.95)
Res2Net (F0)	0.0353(0.0335)	1.17(1.14)
LA ResNet (F0)	0.0388(0.0364)	1.26(1.14)
SE ResNet (F0)	0.0424(0.0392)	1.36(1.23)
ResNet (F0)	0.0493(0.0406)	1.64(1.34)

4.3. Experimental Results on ASVspoof 2019 LA dataset

4.3.1. Effectiveness of the F0 Subband

This section evaluates the effectiveness of F0 subband feature on different network structures. Fig 5 shows the minimal t-DCF and EER results for the different systems we proposed. To avoid randomness in the experiments, the results are averaged for the three runs, with the best of the three runs in parentheses. “F0” represents based on the F0 subband feature, and “L” represents based on the low frequency (0-4000 Hz) Zhang et al. (2021b) subband feature. The first six lines are the results of the F0 subband feature. The last six lines are experimental results based on low frequency subband feature. Fig 6 shows the EER histograms based on the F0 subband and low subband features, with EERs calculated separately for different attack types.

From the Fig 5 and Fig.6, we can see the following.

(1) In the LPS features, the performance of the F0 subband is better than that of the lower subband features in all cases. For example, in our proposed state-of-the-art classifier-SR-LA Res2Net, the average EER of its F0 subband is 0.47%, while the EER of the low subband is 1.86%. Even though the low subband (0-4000Hz) has ten times more band information than F0 (0-400Hz), it performs much worse in the FSD task. This is because the main discriminative information is concentrated in the F0 subband, and the other frequency band information may make it overfitting. The experimental results show that the F0 subband is an important identification feature.

(2) The F0 subband feature has general applicability for different types of attacks. For low subband features, the attack types of A08 (neural waveform), A17 (waveform filtering), and A18 (vocoder) are difficult to detect. It can be seen in the SR-LA Res2Net subgraph that the F0 subband has good performance for different attack types, even for the notorious attack type like A17. Overall, the F0 subband features outperform the lower subbands on different classifiers.

(3) SR-LA Res2Net classifier can fully exploit the discriminatory ability of F0 subbands. For example, from ResNet to SR Res2Net and then to SR-LA Res2Net, attacks such as A08 and A17 are greatly optimized under the F0 subband, but it is more difficult to develop for the low subband, which may be due to the interference of having a lot of redundant information in the low subband.

4.3.2. Effectiveness of the SR-LA Res2Net Architecture

To verify the effectiveness of our proposed FSD system based on the F0 subband and the SR-LA Res2Net, we performed a series of ablation experiments. Table 3 shows the min t-DCF and EER results of our proposed different systems. In addition, to validate the effectiveness of our proposed SR-LA Res2Net, we used some recently published advanced network to model the F0 subband. Table 5 shows the EER and t-DCF for the different networks.

Firstly, the multi-scale feature representation of F0 subband is an effective way to improve the performance of the pseudo-speech detection system. the EER result of "ResNet (F0)" is 1.64%, while the EER result of "Res2Net (F0)" is 1.17%. This is due to the fact that Res2Net is designed with residual connections within the channel group so that the model can learn information at different scales to discriminate. However, when the Res2Net extracts multi-scale features, the larger the number of channel groups, the more information is superimposed, and the spatial structure of the features will also have more artifacts, which affects the ability of the model to capture fundamental discriminative information. Therefore, we design the spatial reconstructed block to be integrated into the residual connections of Res2Net to reconstruct the feature space before transferring the information. Experimental results show that SR-Res2Net (F0) has a good performance improvement over Res2Net (F0). This suggests that the spatial reconstruction mechanism helps remove spatial structure artifacts and further improves the performance of the model.

Next, we integrate a local attention block at the bottom of Res2Net. This is because the deepest channel group of the Res2Net superimposes all the information, and the rest also superimposes a lot of information, which leads to the generation of a lot of redundant information and further covers the important discriminative information. We propose to restore the weights of important information through local attention blocks after this information is aggregated. Specifically, we also compare the performance of local attention (LA) and global attention (SE) Hu et al. (2019), and the experimental results show that local attention is better than global attention. We think there are two reasons: ① When generating the attention map, much long-distance information in the global information cannot accurately capture its specific connection, and the short-distance information can better judge the weight of the central information; ② The global attention block uses two fully connected layers, which are used for dimensionality reduction and expansion, respectively. The

Table 4

EER(%) results for the development subset (A01-A06) and the evaluation subset and the total EER results for the respective subsets. (A07-A19). The EER(%) of each spoof method is calculated separately. Where "A, B, C, D, E, F, G and H" denote the based F0 subband feature SR-LA Res2Net, SR-SE Res2Net, SR Res2Net, LA Res2Net, Res2Net, SE ResNet, LA ResNet and ResNet, respectively. B1 and B2 are based on two baseline systems on ASVspoof 2019 LA.

Systems	Development set							Evaluation set													
								Seen attacks		Unseen attacks											
	A01	A02	A03	A04	A05	A06	Total	A16	A19	A07	A08	A09	A10	A11	A12	A13	A14	A15	A17	A18	Total
A	0.00	0.00	0.00	0.19	0.11	0.19	0.12	0.32	0.50	0.30	0.85	0.04	0.46	0.47	0.09	0.09	0.20	0.66	0.70	0.63	0.47
B	0.07	0.03	0.00	0.31	0.11	0.23	0.23	0.52	0.54	0.24	1.38	0.02	0.48	0.58	0.12	0.05	0.34	0.79	0.93	1.05	0.84
C	0.07	0.07	0.03	0.27	0.07	0.19	0.15	0.44	0.81	0.59	1.62	0.12	0.91	0.59	0.30	0.06	0.14	0.99	1.95	1.42	0.96
D	0.07	0.03	0.00	0.15	0.15	0.13	0.15	0.43	0.75	0.59	1.40	0.13	0.70	0.58	0.28	0.14	0.17	0.89	1.24	1.44	0.80
E	0.11	0.11	0.11	0.11	0.11	0.35	0.19	0.30	0.99	0.38	2.97	0.13	0.52	0.46	0.20	0.10	0.17	0.75	3.09	2.07	1.17
F	0.03	0.03	0.03	0.30	0.19	0.27	0.19	0.48	1.05	0.26	2.58	0.06	0.40	0.40	6.13	0.17	0.22	0.70	2.11	1.72	1.36
G	0.15	0.07	0.07	0.46	0.15	0.19	0.19	0.75	0.93	0.42	1.97	0.02	0.62	0.61	0.26	0.16	0.30	0.77	2.28	1.93	1.26
H	0.07	0.07	0.07	0.46	0.15	0.19	0.19	0.34	2.07	0.20	1.76	0.10	0.36	0.40	0.16	0.10	0.54	0.34	4.43	2.89	1.64
B1	0.00	0.00	0.08	0.00	0.94	0.03	0.43	0.00	0.04	0.00	0.04	0.14	15.16	0.08	4.74	26.15	10.85	1.26	19.62	3.81	9.57
B2	0.03	0.00	0.00	4.90	0.16	5.27	2.71	6.31	13.94	12.86	0.37	0.00	18.97	0.12	4.92	9.57	1.22	2.22	7.71	3.58	8.09

Table 5

Comparison of the results of F0 subband features on other advanced classifiers.

Systems	t-DCF	EER(%)
ACNN (FFT) Ling et al. (2021)	0.0510	1.87
ACNN (F0)	0.0454	1.46
MCG-Res2Net (CQT) Li et al. (2021b)	0.0520	1.78
MCG-Res2Net (F0)	0.0299	1.03

dimensionality reduction operation may result in the loss of some information, which can affect the discriminability of the model. According to the experimental results of integrating local attention blocks and global attention blocks respectively, LA Res2Net achieves an EER result of 0.80%, and SR-LA Res2Net achieves an EER result of 0.47%. This shows that local attention can capture important information in more detail and reduce the influence of redundant information left over from the network.

Finally, for the setting of the number of channel groups in the SR-LA Res2Net, we believe that $n=8$ is most appropriate for right in the fake audio detection task, thus achieving state-of-the-art performance. This is because the information exchange at this time is sufficient and the feature representation is reasonable.

Moreover, to verify the effectiveness of our proposed SR-LA Res2Net, we simulate the F0 subband with some recently published advanced networks. Table 5 shows the EER and t-DCF of different networks, which demonstrates the differences between different networks when using either the original features or the F0 subband. Fig. 7 shows the specific EER results of the attack. From Table 5 and Fig. 7, we see that the F0 subband feature can achieve excellent performance when paired with other networks, and SR-LA

Res2Net can fully access the discriminative information of the F0 subband and perform extremely well in all aspects.

4.3.3. Effective Generalization Ability of SR-LA Res2Net Architecture

In the ASVspoof 2019 LA dataset, most of the evaluation data are unseen spoofing attack algorithms. Fig. 8 shows the dense histogram of the scores of the SR-LA Res2Net (F0) system on the development and evaluation sets, respectively. It can be seen from Fig. 8 that our proposed system has almost perfect discrimination between known attack algorithms, and such discrimination ability is also well generalized to the unseen evaluation set.

In addition, Table 4 also counts the EER and t-DCF of each attack algorithm we propose for different systems. Where B1 and B2 Wang et al. (2020b) are the two baseline systems of ASVspoof 2019 LA, and B1 and B2 are based on the CQCC-GMM and LFCC-GMM methods, respectively. From Table 4, we can draw the following points. First, when different classifiers capture the details of the feature and then generalize to unknown attacks, their biases will be large. For example, the GMM-based baseline algorithm is very effective against attack algorithms such as A08, but the performance of attack algorithms such as A10, A13, A14, and A17 becomes extremely poor. Even so, it is not our original intention to only effectively target a certain attack algorithm. For example, our proposed SR-LA Res2Net ($n=8$, F0) can be generalized to each unseen attack more evenly, which is the focus of our work.

Second, it is well known that the A17 algorithm is notorious, and the method was judged to have the highest spoofing ability in the 2018 Speech Transformation Challenge Kinunen, Lorenzo-Trueba, Yamagishi, Toda, Saito, Villavicencio and Ling (2018). However, our proposed SR-LA Res2Net system can obtain 0.70% EER on the A17 attack,

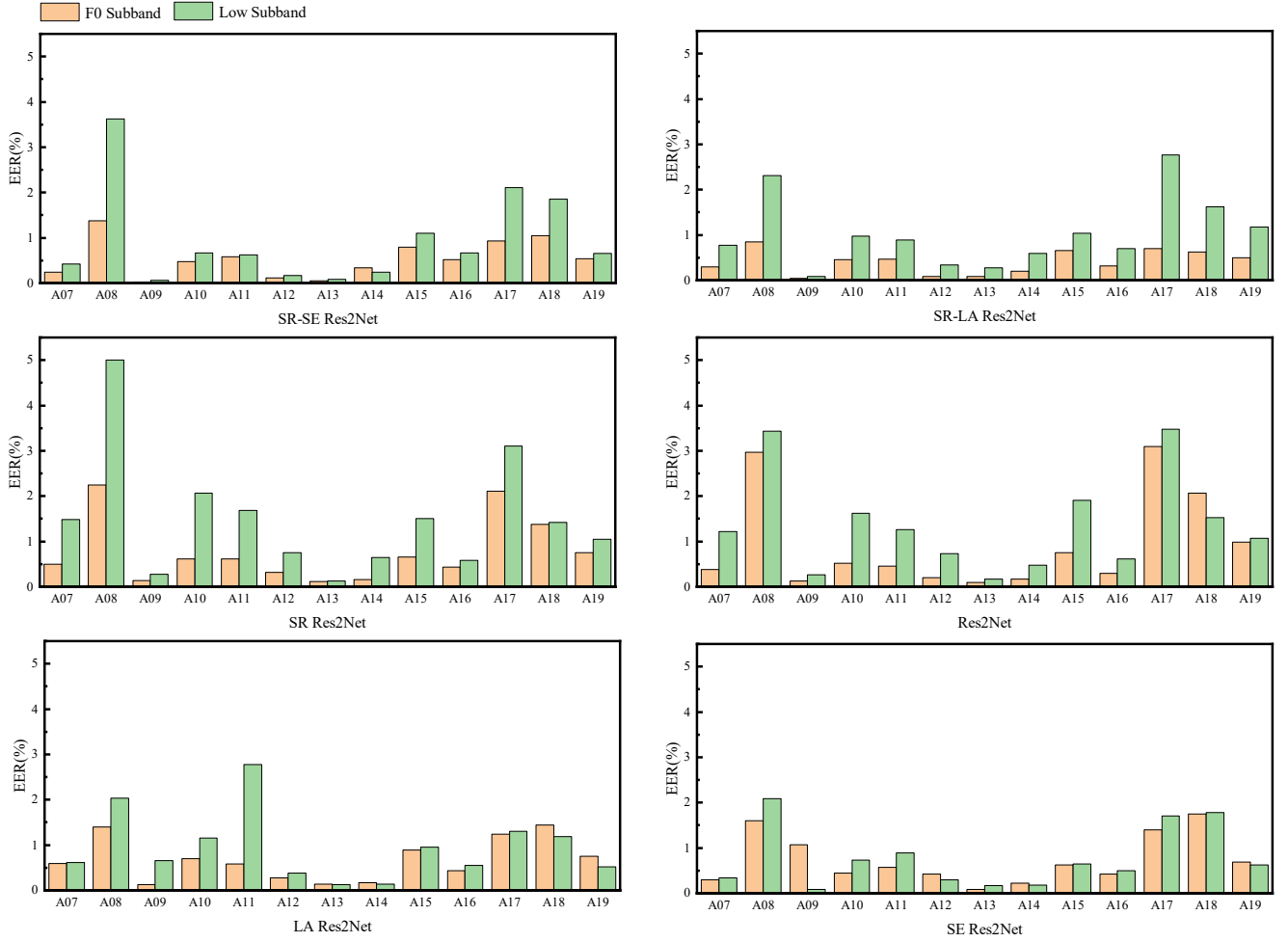


Figure 6: EER results of our proposed different systems on the ASVspoof 2019 LA evaluation set (A07-A19). The EER of each spoof method is calculated separately.

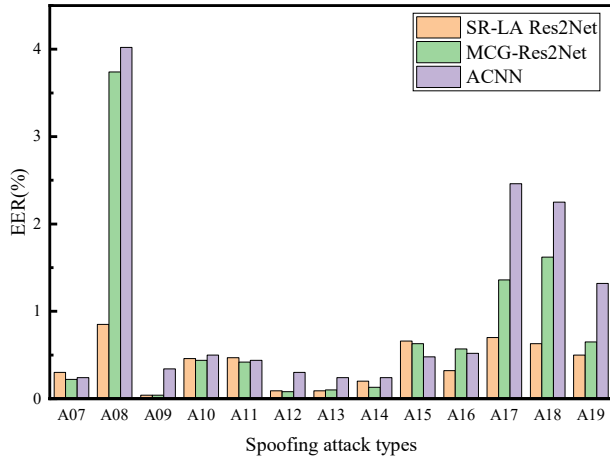


Figure 7: EER results of the F0 subband feature on other advanced classifiers.

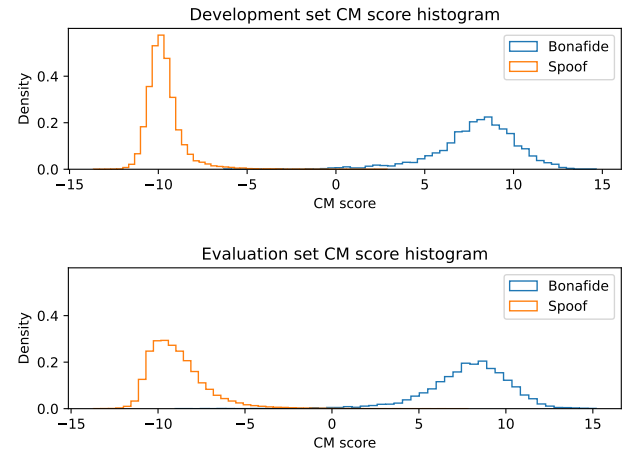


Figure 8: Score density histogram for the SR-LA Res2Net (F0) system based on the ASVspoof 2019 LA development set.

which is the best performance among all systems. We believe that the multi-scale feature representation enables the FSD system to be generalized to spoofing attacks like A17. the EER results of the ResNet (F0) and Res2Net (F0) systems on

A17 are 4.43% and 3.09%, respectively, which indicates that multi-scale features can greatly extend the feature receptive field and enhance its generalizability. However, the channel

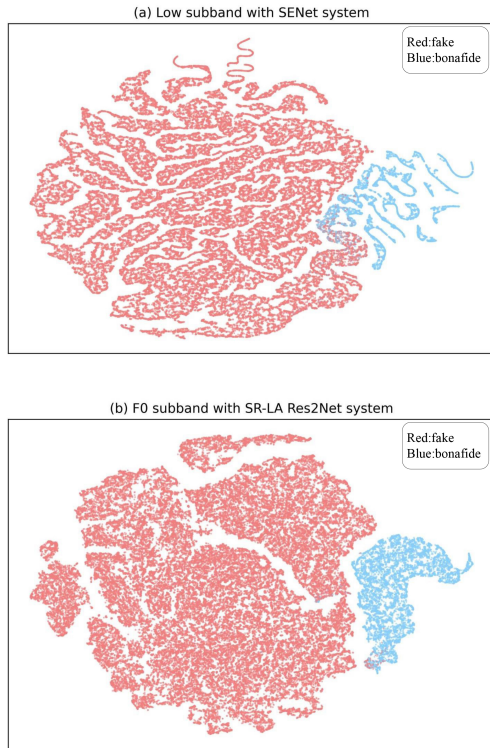


Figure 9: Subplot (a) shows the t-SNE visualization for the low-frequency subband and SENet system, and subplot (b) shows the t-SNE visualization for the F0 subband and SR-LA Res2Net system. The blue dots represent real speech and the red dots represent false speech.

group information of its Res2Net architecture is constantly superimposed, which requires a spatial reconstruction block to reconstruct each channel group information, and the EER result of its SR Res2Net (F0) at A17 is 1.95%, and the experimental results prove that the spatial reconstruction block can reduce the influence of redundant information. In addition, other systems have poor performance for unseen attacks like A08, A17, and A18, but the SR-LA Res2Net (F0) system achieves high performance in the face of all unseen attacks. This further validates the need to integrate spatial reconstruction block and local attention block in Res2Net, which can greatly improve the generalization ability of the model.

Third, compared to our proposed SR-LA Res2Net (F0) system, other systems are difficult to pass in some individual deception algorithms. For example, the B1 system achieves an EER result of 26.15% in the A13 algorithm, and our SR-LA Res2Net (F0) system has an EER of 0.09 for A13, and other systems also performed well. For A18, the SR-LA Res2Net (F0) system leads the way.

In summary, the strong generalization of the SR-LA Res2Net (F0) system comes from the spatial reconstructed block and the local attention block. By reconstructing the feature space and focusing on local information, it reduces the multi-scale sequelae brought by feature representation, which greatly improves the performance of the FSD system.

Table 6

EER and t-DCF of single systems and primary systems based on the top performance of ASVspoof 2019 LA dataset.

(a) Single systems		
System	t-DCF	EER%
CQCC+GMM (B1)	0.2316	9.57
LFCC+GMM (B2)	0.2116	8.09
LFCC-Siamese CNN Lei, Yang, Liu and Ye (2020)	0.0930	3.79
RW-ResNet Ma, Ren and Xu (2021)	0.0820	2.98
Ling et al. Ling et al. (2021)	0.0510	1.87
MCG-Res2Net50 Li et al. (2021b)	0.0520	1.78
FFT-L-SENet Zhang et al. (2021b)	0.0368	1.14
AASIST Jung et al. (2022)	0.0347	1.13
SAMO Ding, Zhang and Duan (2023)	0.0356	1.08
PA-Res2Net Kim and Ban (2023)	0.0300	1.07
ECANet_SD Xue, Fan, Yi, Wang, Wen, Zhang and Lv (2023)	0.0295	0.88
ours (single system)	0.0159	0.47

(b) Fusion systems		
System	t-DCF	EER%
T05 Todisco et al. (2019)	0.0069	0.22
T45 Lavrentyeva, Tseren, Volkova, Gorlanov, Kozlov and Novoselov (2019)	0.0510	1.84
T60 Chettri, Stoller, Morfi, Ramírez, Benetos and Sturm (2019)	0.0755	2.64
GMM fusion Tak, J. Patino, NAutsch, Evans and Todisco (2020)	0.0740	2.92
T24 Todisco et al. (2019)	0.0953	3.45
T50 Yang, Wang, Dinkel, Chen, Wang, Qian and Yu (2019c)	0.1671	3.56
ours (single system)	0.0159	0.47

4.3.4. Comparison with Other Systems

Table 6 shows the results of the eight best-performing single systems, the six main systems, and our best system on the ASVspoof 2019 LA evaluation set, where B1 and B2 are the baseline systems. The results of single systems are shown in Table 6a. These systems include some top-performance systems from the ASVspoof 2019 challenge and systems from recently published papers. Table 6b shows the results of the primary systems, where T05, T45, T60, T24, and T50 represent the anonymous identifiers of the teams in the ASVspoof 2019 challenge. These primary systems may contain multiple front-end features and neural network architectures. The GMM fusion system consists of the nonlinear fusion of its six subbands. From the performance comparison of different systems in Table 6, it can be seen that our proposed system achieves state-of-the-art performance in a single system, and also outperforms the

Table 7

EER and t-DCF of single systems and primary systems based on the top performance of ASVspoof 2021 LA dataset.

(a) Single systems		
System	t-DCF	EER%
B03 Yamagishi et al. (2021)	0.3445	9.26
B04 Yamagishi et al. (2021)	0.4257	9.50
B01 Yamagishi et al. (2021)	0.4974	15.62
B02 Yamagishi et al. (2021)	0.5758	19.30
ours (single system)	0.2642	3.61

(b) Fusion systems		
System	t-DCF	EER%
T23 Tomilov, Svishchev, Volkova, Chirkovskiy, Kondratev and Lavrentyeva (2021)	0.2177	1.32
T20 Chen, Khoury, Phatak and Sivaraman (2021)	0.2608	3.21
T04 Cáceres, Font, Grau and Molina (2021)	0.2747	5.58
T06 Kang, Alam and Fathan (2021)	0.2853	5.66
ours (single system)	0.2642	3.61

second-ranked system on the ASVspoof 2019 LA challenge among the primary systems.

To the best of our knowledge, among all fusion systems, only the T05 system outperforms us. Here we want to emphasize that the fusion system is obtained by fusing multiple single systems, which means that multiple models need to be trained and finally fused, so that the overall model parameters are huge. Moreover, T05 is a fusion of 7 single systems, including 2 Resnet models, 4 MobileNet models, and 1 DenseNet model, and the final results are obtained by combining the equal weights of these 7 single systems. It can be seen that the T05 system architecture is extremely complex. Therefore, our proposed single system has advantages in terms of performance and network architecture.

4.3.5. *t*-SNE Visualization Analysis

To visualize the effectiveness of the proposed approach, we also visualize the baseline system and my proposed system using *t*-SNE van der Maaten and Hinton (2008), respectively. Both models are trained on the LA dataset in Asvspoof 2019 and take the penultimate layer of the network. As shown in Fig. 9, we can see that the real and fake speech of the Low subband and SENet systems are not distinguished, and there are many blue dots embedded inside the red dots. While the true and false speech of the F0 subband and SR-LA Res2Net systems are separated, there is only a little blending at the boundary. The above visualization results further validate our experimental results.

4.4. Experimental Results on ASVspoof 2021 LA dataset

Table 7 shows the results of the ASVspoof 2021 LA Challenge for single and fusion systems. Among them, the T23 Tomilov et al. (2021) system is a fusion of twelve subsystems, including ten MSTFT-LCNN systems, one MSTFT-ResNet system, and one RawNet system, finally fused in the scoring stage by a fine weight assignment; the T20Chen et al. (2021) system is a fusion of three subsystems based on ResNet system with equal weight fusion of scoring; the T04Cáceres et al. (2021) system is a scoring fusion of three subsystems, namely LFCC-LCNN, RawNet2, and lightweight TDNN Focal, and all three subsystems use a data enhancement strategy; the T06Kang et al. (2021) system is a fusion of eight subsystems, namely an LFCC-LCNN system (baseline), one RawNet2 system (baseline), one LFCC-GMM, four LFCC-SENet systems, and one PSCC-TDNN system, all of which use data enhancement strategies except for the baseline system. B01-B04 are the four baseline systems for the ASVspoof 2021 LA Challenge. The following points can be observed from the table:

(1) Most of the systems perform data enhancement in the face of transmission interference in the ASVspoof 2021 LA data set, and the performance is poor for the baseline systems that do not perform data enhancement.

(2) Several of the most advanced systems submitted at the ASVspoof 2021 LA challenge are fusion systems, while we can obtain good performance for our single system.

In conclusion, our proposed single system is competitive in the face of both single and fusion systems, which further validates the effectiveness of our proposed method.

5. Discussions

The above experimental results show that our proposed F0 subband with SR-LA Res2Net is very effective for FSD. We can make the following interesting observations.

Our proposed F0 subband feature has a strong discriminative ability in distinguishing real and fake speech. Compared with the low subband, the proposed F0 subband can obtain better FSD results. The reason is that the F0 value in synthetic speech is difficult to predict, and the F0 is relatively smooth, which may have a large degree of mismatch with the F0 of real speech. Therefore, we use the frequency band that contains most of F0, which can better utilize the discriminative information of F0.

SR-LA Res2Net can further exploit the multi-scale discriminative information of F0 and improve the performance of FSD. Compared with Res2Net, the proposed SR-LA Res2Net can effectively reduce the influence of masked information. The reason is that the SR block can re-integrate the spatial information of the channel group, thereby reducing the interference of redundant feature structures. The LA block aims to focus on local information and removes redundant information. Therefore, our proposed method can further enhance the multi-scale feature representation.

Moreover, from the results of ASVspoof 2021 LA database we can find that our proposed single system can acquire competitive performance in terms of fusion systems, which indicates that the F0 subband features can distinguish well between real and fake speech, and the SR-LA Res2Net can further obtain the discriminative information of F0 subband.

In summary, the proposed F0 subband with SR-LA Res2Net can effectively distinguish the real and fake speech so that it can improve the performance of FSD.

6. Conclusions

In this paper, we propose a F0 subband with SR-LA Res2Net for FSD. The F0 distribution of synthetic speech is too smooth so that it is very different from the real one. Therefore, we think the F0 contains the discriminative information. In addition, to effectively model the F0 subband, we propose a novel SR-LA Res2Net for FSD. Specifically, the SR block is designed to eliminate spatial artifacts when information is transmitted between channel groups. The LA block is used to focus on local information. Experimental results on the ASVspoof 2019 LA dataset show that our proposed approach is very effective against unseen spoofing attacks and achieves a minimum t-DCF of 0.0159 and an EER of 0.47%, which achieves the state-of-the-art performance among all single systems. One of the limitations of this work is that we only use the F0 subband for FSD. The other speech information is abandoned, which may also contain some important discriminative information. In the future, to make full use of the speech information, we will explore to combine the F0 subband with other speech features to further improve the performance of FSD.

7. Acknowledgements

This work is supported by the STI 2030—Major Projects (No.2021ZD0201500), the National Natural Science Foundation of China (NSFC) (No.62201002, No.61972437), Excellent Youth Foundation of Anhui Scientific Committee (No.208085J05), Special Fund for Key Program of Science and Technology of Anhui Province (No.202203a07020008), the Open Research Projects of Zhejiang Lab (NO.2021KH0AB06) and the Open Projects Program of National Laboratory of Pattern Recognition (NO.202200014).

References

- Ali, M., Sabir, A., Hassan, M., 2021. Fake audio detection using hierarchical representations learning and spectrogram features, in: 2021 International Conference on Robotics and Automation in Industry (ICRAI), IEEE. pp. 1–6.
- Chen, T., Khoury, E., Phatak, K., Sivaraman, G., 2021. Pindrop labs' submission to the asvspoof 2021 challenge, in: Proc. 2021 Edition of the Automatic Speaker Verification and Spoofing Countermeasures Challenge, pp. 89–93.
- Chen, T., Kumar, A., Nagarsheth, P., Sivaraman, G., Khoury, E., 2020. Generalization of audio deepfake detection, in: Proc. Odyssey 2020 The Speaker and Language Recognition Workshop, pp. 132–137.
- Chettri, B., Kinnunen, T., Benetos, E., 2020a. Subband modeling for spoofing detection in automatic speaker verification, in: Proceedings of Odyssey 2020: The Speaker and Language Recognition Workshop, ISCA. pp. 341–348.
- Chettri, B., Kinnunen, T., Benetos, E., 2020b. Subband modeling for spoofing detection in automatic speaker verification, in: Proc. Odyssey 2020 The Speaker and Language Recognition Workshop, pp. 341–348.
- Chettri, B., Stoller, D., Morfi, V., Ramírez, M., Benetos, E., Sturm, B., 2019. Ensemble models for spoofing detection in automatic speaker verification, in: Proc. Interspeech, pp. 1018–1022.
- Cáceres, J., Font, R., Grau, T., Molina, J., 2021. The biometric vox system for the asvspoof 2021 challenge, in: Proc. 2021 Edition of the Automatic Speaker Verification and Spoofing Countermeasures Challenge, pp. 68–74.
- Das, R.K., Yang, J., Li, H., 2019. Long range acoustic features for spoofed speech detection., in: Interspeech, pp. 1058–1062.
- Ding, S., Zhang, Y., Duan, Z., 2023. Samo: Speaker attractor multi-center one-class learning for voice anti-spoofing, in: ICASSP 2023-2023 IEEE International Conference on Acoustics, Speech and Signal Processing (ICASSP), IEEE. pp. 1–5.
- Doan, T.P., Nguyen-Vu, L., Jung, S., Hong, K., 2023. Bts-e: Audio deepfake detection using breathing-talking-silence encoder, in: ICASSP 2023-2023 IEEE International Conference on Acoustics, Speech and Signal Processing (ICASSP), IEEE. pp. 1–5.
- Gao, S., Cheng, M.M., Zhao, K., Zhang, X.Y., Yang, M.H., Torr, P.H., 2019. Res2net: a new multi-scale backbone architecture. IEEE transactions on pattern analysis and machine intelligence , 652–662.
- Hajipour, M., Akhaee, M.A., Toosi, R., 2021. Listening to sounds of silence for audio replay attack detection, in: 2021 7th International Conference on Signal Processing and Intelligent Systems (ICSPIS), IEEE. pp. 1–6.
- He, J., Xu, J., Zhang, L., Zhu, J., 2023. An interpretive constrained linear model for resnet and mgnet. Neural Networks 162, 384–392.
- He, K., Zhang, X., Ren, S., Sun, J., 2016. Deep residual learning for image recognition, in: 2016 IEEE Conference on Computer Vision and Pattern Recognition (CVPR), IEEE. pp. 770–778.
- Hu, J., Shen, L., Albanie, S., Sun, G., Wu, E., 2019. Squeeze-and-excitation networks. IEEE Transactions on Pattern Analysis and Machine Intelligence 42, 2011–2023.
- Huang, B., Cui, S., Huang, J., Kang, X., 2023. Discriminative frequency information learning for end-to-end speech anti-spoofing. IEEE Signal Processing Letters 30, 185–189.
- Huang, S.F., Lin, C.J., Liu, D.R., Chen, Y.C., Lee, H.y., 2022. Meta-tts: Meta-learning for few-shot speaker adaptive text-to-speech. IEEE/ACM Transactions on Audio, Speech, and Language Processing 30, 1558–1571.
- Jung, J.w., Heo, H.S., Tak, H., Shim, H.j., Chung, J.S., Lee, B.J., Yu, H.J., Evans, N., 2022. Aasist: audio anti-spoofing using integrated spectro-temporal graph attention networks, in: ICASSP 2022-2022 IEEE International Conference on Acoustics, Speech and Signal Processing (ICASSP), IEEE. pp. 6367–6371.
- Kang, W.H., Alam, J., Fathan, A., 2021. Crim's system description for the asvspoof2021 challenge, in: Proc. 2021 Edition of the Automatic Speaker Verification and Spoofing Countermeasures Challenge, pp. 100–106.
- Kim, J., Ban, S.M., 2023. Phase-aware spoof speech detection based on res2net with phase network, in: ICASSP 2023-2023 IEEE International Conference on Acoustics, Speech and Signal Processing (ICASSP), IEEE. pp. 1–5.
- Kinnunen, T., Lorenzo-Trueba, J., Yamagishi, J., Toda, T., Saito, D., Villavicencio, F., Ling, Z., 2018. A spoofing benchmark for the 2018 voice conversion challenge: Leveraging from spoofing countermeasures for speech artifact assessment, in: The Speaker and Language Recognition Workshop, ISCA. pp. 187–194.
- Kinnunen, T., Sahidullah, M., Delgado, H., Todisco, M., Evans, N., Yamagishi, J., Lee, K.A., 2017a. The ASVspoof 2017 challenge: assessing the limits of replay spoofing attack detection, in: Proc. Interspeech, pp. 2–6.

- Kinnunen, T., Sahidullah, M., Falcone, M., Costantini, L., Hautamäki, R.G., Thomsen, D., Sarkar, A., Tan, Z.H., Delgado, H., Todisco, M., et al., 2017b. Reddotts replayed: a new replay spoofing attack corpus for text-dependent speaker verification research, in: 2017 IEEE International conference on acoustics, speech and signal processing (ICASSP), IEEE. pp. 5395–5399.
- Kinnunen, T., Wu, Z.Z., Lee, K.A., Sedlak, F., Chng, E.S., Li, H., 2012. Vulnerability of speaker verification systems against voice conversion spoofing attacks: The case of telephone speech, in: 2012 IEEE International Conference on Acoustics, Speech and Signal Processing (ICASSP), IEEE. pp. 4401–4404.
- Łańcucki, A., 2021. Fastpitch: Parallel text-to-speech with pitch prediction, in: IEEE International Conference on Acoustics, Speech and Signal Processing (ICASSP), IEEE. pp. 6588–6592.
- Lavrentyeva, G., Tseren, A., Volkova, M., Gorlanov, A., Kozlov, A., Novoselov, S., 2019. Stc antispoofing systems for the asvspoof2019 challenge, in: Proc. Interspeech, pp. 1033–1037.
- Lei, Z., Yang, Y., Liu, C., Ye, J., 2020. Siamese convolutional neural network using gaussian probability feature for spoofing speech detection, in: Proc. Interspeech, pp. 1116–1120.
- Li, J., Wang, H., He, P., Abdullahi, S.M., Li, B., 2022. Long-term variable q transform: A novel time-frequency transform algorithm for synthetic speech detection. *Digital Signal Processing* 120, 103256.
- Li, X., Li, N., Weng, C., Liu, X., Su, D., Yu, D., Meng, H., 2021a. Replay and synthetic speech detection with res2net architecture, in: IEEE International Conference on Acoustics, Speech and Signal Processing (ICASSP), IEEE. pp. 6354–6358.
- Li, X., Wu, X., Lu, H., Liu, X., Meng, H., 2021b. Channel-wise gated res2net: towards robust detection of synthetic speech attacks. *Proc. Interspeech* 2021.
- Ling, H., Huang, L., Huang, J., Zhang, B., Li, P., 2021. Attention-based convolutional neural network for asv spoofing detection, in: Proc. Interspeech, pp. 4289–4293.
- Lv, Z., Zhang, S., Tang, K., Hu, P., 2022. Fake audio detection based on unsupervised pretraining models, in: ICASSP 2022-2022 IEEE International Conference on Acoustics, Speech and Signal Processing (ICASSP), IEEE. pp. 9231–9235.
- Ma, Y., Ren, Z., Xu, S., 2021. Rw-resnet: a novel speech anti-spoofing model using raw waveform, in: Proc. Interspeech, pp. 4144–4148.
- van der Maaten, L., Hinton, G., 2008. Visualizing data using t-sne. *Journal of Machine Learning Research* 9.
- Paul, A., Das, R.K., Sinha, R., Prasanna, S.M., 2016. Countermeasure to handle replay attacks in practical speaker verification systems, in: 2016 International Conference on Signal Processing and Communications (SPCOM), IEEE. pp. 1–5.
- Paul, D., Pal, M., Saha, G., 2017. Spectral features for synthetic speech detection. *IEEE journal of selected topics in signal processing* 11, 605–617.
- Sanchez, J., Saratxaga, I., Hernaez, I., Navas, E., Erro, D., Raitio, T., 2015. Toward a universal synthetic speech spoofing detection using phase information. *IEEE Transactions on Information Forensics and Security* 10, 810–820.
- Shang, W., Stevenson, M., 2008. A preliminary study of factors affecting the performance of a playback attack detector, in: 2008 Canadian Conference on Electrical and Computer Engineering, IEEE. pp. 459–464.
- Shchemelinin, Vadim, Simonchik, K., 2013. Examining vulnerability of voice verification systems to spoofing attacks by means of a tts system, in: Proceedings of the 15th International Conference on Speech and Computer-Volume 8113, pp. 132–137.
- Sun, T., Ding, S., Guo, L., 2022. Low-degree term first in resnet, its variants and the whole neural network family. *Neural Networks* 148, 155–165.
- Tak, H., J. Patino, N. Autsch, A., Evans, N., Todisco, M., 2020. Spoofing attack detection using the non-linear fusion of sub-band classifiers, in: Proc. Interspeech, pp. 1106–1110.
- Tak, H., weon Jung, J., Patino, J., Todisco, M., Evans, N., 2021a. Graph attention networks for anti-spoofing, in: Proc. Interspeech 2021, pp. 2356–2360.
- Tak, H., Jung, J.W., Patino, J., Kamble, M., Todisco, M., Evans, N., 2021b. End-to-end spectro-temporal graph attention networks for speaker verification anti-spoofing and speech deepfake detection, in: ASVspoof 2021, automatic speaker verification and spoofing countermeasures challenge, ISCA. pp. 1–8.
- Tak, H., Kamble, M., Patino, J., Todisco, M., Evans, N., 2022. Rawboost: A raw data boosting and augmentation method applied to automatic speaker verification anti-spoofing, in: ICASSP 2022-2022 IEEE International Conference on Acoustics, Speech and Signal Processing (ICASSP), IEEE. pp. 6382–6386.
- Tian, X., Lee, S.W., Wu, Z., Chng, E.S., Li, H., 2017. An exemplar-based approach to frequency warping for voice conversion. *IEEE/ACM Transactions on Audio, Speech, and Language Processing* 25, 1863–1876.
- Todisco, M., Wang, X., Vestman, V., Sahidullah, M., Delgado, H., Nautsch, A., Yamagishi, J., Evans, N., Kinnunen, T.H., Lee, K.A., 2019. ASVspoof 2019: future horizons in spoofed and fake audio detection, in: Proc. Interspeech, pp. 1008–1012.
- Tomilov, A., Svishchev, A., Volkova, M., Chirkovskiy, A., Kondratev, A., Lavrentyeva, G., 2021. Stc antispoofing systems for the asvspoof2021 challenge, in: Proc. 2021 Edition of the Automatic Speaker Verification and Spoofing Countermeasures Challenge, pp. 61–67.
- Wang, Q., Wu, B., Zhu, P., Li, P., Zuo, W., Hu, Q., 2020a. Eca-net: Efficient channel attention for deep convolutional neural networks. 2020 IEEE/CVF Conference on Computer Vision and Pattern Recognition (CVPR), 11531–11539.
- Wang, X., Yamagishi, J., Todisco, M., Delgado, H., Nautsch, A., Evans, N., Sahidullah, M., Vestman, V., Kinnunen, T., Lee, K.A., et al., 2020b. Asvspoof 2019: A large-scale public database of synthesized, converted and replayed speech. *Computer Speech & Language* 64, 101114.
- Wei, L., Long, Y., Wei, H., Li, Y., 2022. New acoustic features for synthetic and replay spoofing attack detection. *Symmetry* 14, 274.
- Williams, J., Rownicka, J., 2019. Speech replay detection with x-vector attack embeddings and spectral features. *Proc. Interspeech* 2019, 1053–1057.
- Witkowski, M., Kacprzak, S., Zelasko, P., Kowalczyk, K., Galka, J., 2017. Audio replay attack detection using high-frequency features., in: Interspeech, pp. 27–31.
- Woo, S., Park, J., Lee, J.Y., Kweon, I.S., 2018. Cbam: Convolutional block attention module, in: Proceedings of the European conference on computer vision (ECCV), pp. 3–19.
- Wu, Z., Kinnunen, T., Evans, N., Yamagishi, J., Hanilci, C., Sahidullah, M., Sizov, A., 2015. ASVspoof 2015: the first automatic speaker verification spoofing and countermeasures challenge, in: Proc. Interspeech, pp. 2037–2041.
- Xue, J., Fan, C., Yi, J., Wang, C., Wen, Z., Zhang, D., Lv, Z., 2023. Learning from yourself: A self-distillation method for fake speech detection, in: ICASSP 2023-2023 IEEE International Conference on Acoustics, Speech and Signal Processing (ICASSP), IEEE. pp. 1–5.
- Yamagishi, J., Wang, X., Todisco, M., Sahidullah, M., Patino, J., Nautsch, A., Liu, X., Lee, K.A., Kinnunen, T., Evans, N., et al., 2021. Asvspoof 2021: accelerating progress in spoofed and deepfake speech detection, in: ASVspoof 2021 Workshop-Automatic Speaker Verification and Spoofing Countermeasures Challenge.
- Yang, J., Das, R.K., 2020. Long-term high frequency features for synthetic speech detection. *Digital Signal Processing* 97, 102622.
- Yang, J., Das, R.K., Li, H., 2019a. Significance of subband features for synthetic speech detection. *IEEE Transactions on Information Forensics and Security* 15, 2160–2170.
- Yang, J., Das, R.K., Zhou, N., 2019b. Extraction of octave spectra information for spoofing attack detection. *IEEE/ACM Transactions on Audio, Speech, and Language Processing* 27, 2373–2384.
- Yang, Y., Wang, H., Dinkel, H., Chen, Z., Wang, S., Qian, Y., Yu, K., 2019c. The sju robust anti-spoofing systems for the asvspoof 2019 challenge, in: Proc. Interspeech, pp. 1038–1042.
- Yi, J., Fu, R., Tao, J., Nie, S., Ma, H., Wang, C., Wang, T., Tian, Z., Bai, Y., Fan, C., et al., 2022. Add 2022: the first audio deep synthesis detection challenge, in: ICASSP 2022-2022 IEEE International Conference on

- Acoustics, Speech and Signal Processing (ICASSP), IEEE. pp. 9216–9220.
- Zhang, Y., Jiang, F., Duan, Z., 2021a. One-class learning towards synthetic voice spoofing detection. *IEEE Signal Processing Letters*, 937–941.
- Zhang, Y., Wang, W., Zhang, P., 2021b. The effect of silence and dual-band fusion in anti-spoofing system, in: *Proc. Interspeech*, pp. 4279–4283.
- Zhang, Z., Gu, Y., Yi, X., Zhao, X., 2022. Fmfcc-a: a challenging mandarin dataset for synthetic speech detection, in: *Digital Forensics and Watermarking: 20th International Workshop, IWDW 2021, Beijing, China, November 20–22, 2021, Revised Selected Papers*, Springer. pp. 117–131.
- Zhang, Z., Yi, X., Zhao, X., 2021c. Fake speech detection using residual network with transformer encoder, in: *Proceedings of the 2021 ACM workshop on information hiding and multimedia security*, pp. 13–22.